NeuroImage: Clinical 37 (2023) 103353

Contents lists available at ScienceDirect

NeuroImage: Clinical

journal homepage: www.elsevier.com/locate/ynicl

MRI histogram analysis of tumor-infiltrating CD8+ T cell levels in patients with glioblastoma

Caiqiang Xue [a,b,c,d,1], Qing Zhou [a,b,c,d,1], Peng Zhang [e], Bin Zhang [a,b,c,d], Qiu Sun [a,b,c,d], Shenglin Li [a,b,c,d], Juan Deng [a,b,c,d], Xianwang Liu [a,b,c,d], Junlin Zhou [a,b,c,d,*]

[a] Department of Radiology, Lanzhou University Second Hospital, Cuiyingmen No. 82, Chengguan District, Lanzhou 730030, China
[b] Second Clinical School, Lanzhou University, Lanzhou, China
[c] Key Laboratory of Medical Imaging of Gansu Province, Lanzhou, China
[d] Gansu International Scientific and Technological Cooperation Base of Medical Imaging Artificial Intelligence, Lanzhou, China
[e] Department of Pathology, Lanzhou University Second Hospital, Cuiyingmen No. 82, Chengguan District, Lanzhou 730030, China

ARTICLE INFO

Keywords:
Glioblastoma
Magnetic resonance imaging
Histogram analysis
CD8+ T cells
Tumor microenvironment

ABSTRACT

Objective: To investigate the utility of preoperative magnetic resonance imaging histogram analysis for evaluating tumor-infiltrating CD8+ T cells in patients with glioblastoma (GBM).

Methods: We retrospectively analyzed the pathological and imaging data of 61 patients with GBM confirmed by surgery and pathology. Moreover, the levels of tumor-infiltrating CD8+ T cells in tumor tissue samples obtained from the patients were quantified through immunohistochemical staining and evaluated with respect to overall survival. The patients were divided into the high and low CD8 expression groups. Preoperative T1-weighted contrast-enhanced (T1C) histogram parameters of patients with GBM were extracted using Firevoxel software. We investigated the correlation between the histogram feature parameters and CD8+ T cells. We performed statistical analyses of the T1C histogram parameters in both groups and identified characteristic parameters with significant between-group differences. Additionally, we performed a receiver operating characteristic curve (ROC) analysis to determine the predictive utility of these parameters.

Results: The levels of tumor-infiltrating CD8+ T cells were positively associated with overall survival in patients with GBM ($P = 0.0156$). Among the T1C histogram features, the mean, 5th, 10th, 25th, and 50th percentiles were negatively correlated with the levels of CD8+ T cells. Moreover, the coefficient of variation (CV) was positively correlated with the levels of CD8+ T cells (all $P < 0.05$). There was a significant between-group difference in the CV, 1st, 5th, 10th, 25th, and 50th percentiles (all $p < 0.05$). The ROC curve analysis revealed that the CV had the highest AUC value (0.783; 95% confidence interval: 0.658–0.878), with sensitivity and specificity values of 0.784 and 0.750, respectively, for distinguishing between the groups.

Conclusions: The preoperative T1C histogram have additional value for the levels of tumor-infiltrating CD8+ T cells in patients with GBM.

1. Introduction

Glioblastoma (GBM) is the most common malignant brain tumor and has a median overall survival (OS) of 12–18 months (Davis, 2016). The current standard of care for newly diagnosed GBM includes maximal surgical resection, concurrent radiation therapy, and temozolomide (TMZ), followed by adjuvant/maintenance TMZ (Hagiwara et al., 2022). However, currently available treatments allow limited improvement of clinical outcomes in patients with GBM (Sun et al., 2021). Recent novel immunotherapies have demonstrated promising results in various solid

Abbreviations: GBM, Glioblastoma; T1C, T1-weighted contrast-enhanced; CV, Coefficient of variation; TMZ, Temozolomide; TME, Tumor microenvironment; ROI, Region of interest; TR, Retention time; TE, Echo time; T2WI, T2-weighted imaging; OS, Overall survival; SD, Standard deviation; ICC, Intra-class correlation coefficient; ROC, Receiver operating characteristic; AUC, Area under the receiver operating characteristic curve; CI, Confidence interval; TME, Tumor immune microenvironment.

* Corresponding author at: Department of Radiology, Lanzhou University Second Hospital, Cuiyingmen No. 82, Chengguan District, Lanzhou 730030, China.
E-mail address: ery_zhoujl@lzu.edu.cn (J. Zhou).

[1] Caiqiang Xue and Qing Zhou equally contributed to this work.

https://doi.org/10.1016/j.nicl.2023.103353
Received 11 August 2022; Received in revised form 5 February 2023; Accepted 14 February 2023
Available online 18 February 2023

tumors, including melanoma, lymphoma, head and neck cancer, clear cell renal cancer, gastric cancer, bladder cancer, and non-small cell lung cancer (Ren et al., 2021). Immunotherapy has significantly altered the management patterns and strategies for malignant tumors. However, only a small proportion of patients with GBM respond to current immunotherapy treatments (Liu et al., 2022a). The efficacy of GBM immunotherapy is influenced by tumor or tumor microenvironment (TME) factors, including tumor cells, stromal cells, immune cells, and other TME-related factors (Zhou et al., 2020). Specifically, GBM immunotherapy can be negatively affected by the complex interactions between tumor and immune cells within the TME as well as the evasion of host immune responses by glioma cells (Ghouzlani et al., 2021; Lakin et al., 2017). It is important to elucidate the interaction mechanisms underlying various TME components and the mechanism underlying immune escape to further improve current immunotherapy or develop new therapeutic approaches (Ugel et al., 2021).

CD8 is a transmembrane glycoprotein mainly expressed on the surface of cytotoxic T lymphocytes (Bian et al., 2022). CD8+ lymphocytes limit tumor cell growth, inhibit tumor infiltration, and mediate tumor elimination (Apetoh et al., 2015). Therefore, CD8+ T cell infiltration in tumors is a powerful predictor of the clinical and postoperative prognosis of patients (Bian et al., 2021; Teng et al., 2015). Furthermore, intratumoral CD8+ T cell infiltration is associated with better survival in patients with glioma (Han et al., 2014; Yang et al., 2010). Accordingly, there are intervention measures for promoting the dominance of CD8+ T cells in patients with GBM (Feng et al., 2022). However, postoperative pathological examination remains the only assessment method for tumor-infiltrating CD8+ T cells. Therefore, preoperative assessment of tumor-infiltrating CD8+ T cells is necessary for informing the treatment strategies and prognosis of patients with GBM.

Histogram analysis is a post-processing technique for measuring several parameters. It compiles each voxel within a region of interest (ROI) into a histogram that can provide information regarding tumor homogeneity/heterogeneity (Xue et al., 2022). Histogram analysis can better elucidate the tissue microstructure compared with traditional methods using only ROI-based analysis (Xu et al., 2021). There has been increasing interest in histogram analysis, which has been used for grading, molecular typing, differential diagnosis, and prognostic evaluation of gliomas (Gao et al., 2022; Jiang et al., 2022; Ulyte et al., 2016; Zhang et al., 2020). However, the relationship between histograms and tumor-infiltrating CD8+ T cells in patients with GBM remains unclear. We aimed to investigate the predictive utility of preoperative T1C histograms for the levels of tumor-infiltrating CD8+ T cells in patients with GBM.

2. Materials and methods

2.1. Study design and patients

This retrospective study was approved by the local institutional review board, which waived the requirement for informed consent. According to the 2021 World Health Organization (WHO) classifcation of central nervous system tumors, we searched the picture archiving and communication system for patients with GBM who underwent magnetic resonance imaging (MRI) evaluation between January 2018 and January 2021. The inclusion criteria were as follows: (I) no biopsy or drug therapy was performed on the lesion before MRI scan; (II) the lesion was confirmed by histopathological and immunohistochemical examination of the specimen obtained from excisional biopsy. We excluded patients from the initial search results based on the following exclusion criteria: (I) patients who were lost to follow-up; (II) did not undergo immunohistochemical CD8 staining; (III) did not undergo MRI scan 1 week prior to surgery or were incompletely sequenced patients; (IV) ROI delineation could not be performed.. Finally, we included 61 patients (mean age: 52.33 [range: 26–71] years).

2.2. MRI protocol

Head MRI and enhanced scanning were performed using Siemens Verio 3.0 T superconducting MRI scanner with the patients placed in a supine position. The scanning parameters for T1-weighted imaging (T1WI) (gradient echo sequence) were as follows: retention time (TR), 550 ms; echo time (TE), 11 ms; layer thickness, 5.0 mm; layer interval, 1.5 mm; field of view, 260 mm × 260 mm; matrix size, 256 × 256. The parameters for T2-weighted imaging (T2WI) (turbo spin-echo sequence) were as follows: TR, 2200 ms; TE, 96 ms; echo time, 10 ms; echo chain length, 8; excitation number, 2. Gd-DTPA was used to perform enhanced scanning ([Bayer Schering Pharma AG, Berlin, Germany]/kg) with intravenous administration of a contrast agent via a bolus injection of 0.1 mmol/kg at a flow rate of 3.0 ml/s.

2.3. Histopathological analysis

Surgical specimens of the glioblastomas were used for histopathological analysis. An antibody for CD8 (CAL66, 1:100; Abcam, Cambridge, UK) was used for pathology. Each section immunohistochemically stained for CD8 was converted into a digital pathology image (whole slide imaging [WSI], 40x magnification) using the TG Tissue FAXS Plus digital pathology analysis system (TissueGnostics, Austria). Based on the WSI for each CD8, five different high-power fields were randomly segmented and visually assessed by a neuropathologist. The number of CD8+ tumor-infiltrating lymphocytes per photo was manually counted three times per photo by an independent neuropathologist with 15 years of experience. The number was rechecked after a period to ensure repeatability. In case of significant discrepancies in the count, the scores were reassessed to achieve a consistent score.

2.4. Patient grouping

The deaths and deaths attributed to other causes were set as events and censored observations, respectively. Survival time was calculated from the date of surgery to death or the end of follow-up (February 1, 2022). The X-tile program automatically determines the optimal cutoff value based on the smallest p-value obtained using Kaplan-Meier survival analysis and the log-rank test. Accordingly, we used the X-tile program to determine the optimal cutoff CD8 level, which was used to classify the low and high CD8 expression groups.

2.5. Image analysis

Two radiologists (with 7 and 5 years of experience, respectively, in MRI diagnosis of GBM) imported images in the Dicom format into Firevoxel (current version: 387B, NYU School of Medicine, NY, https://wp.nyu.edu/firevoxel/ downloads/), which can run stably under Windows 10, to independently analyze the entire lesion. Subsequently, the largest lesion slice was selected. Based on the T1WI and T2WI images, two radiologists manually traced the ROIs in all 61 GBM margin along the axial T1C without the surrounding brain tissue, and oedema (Figs. 1 and 2). To better assess tumor heterogeneity, the ROI should encompass all tumor information at each level, including necrosis and cystic differentiation (Vajapeyam et al., 2022). Additionally, the ROI outlined area should be slightly smaller than the visible tumor boundary, considering the effect of partial volume effects (Liu et al., 2022b). The outlined area was filled with red, and the software automatically generated a grayscale histogram of the ROI. Histogram analysis was performed using the largest slices to obtain the following histogram parameters: maximum, minimum, mean, standard deviation (SD), variance, coefficient of variation (CV), skewness, kurtosis, entropy, and 1st–99th percentiles. Inter-observer repeatability of the measured histogram parameters was assessed by examining data measured by two radiologists.

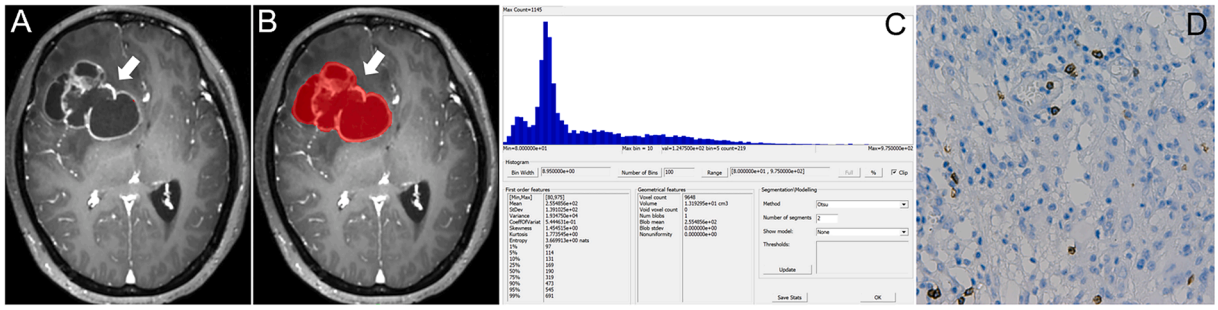

Fig. 1. A 45-year-old woman with right frontal GBM (High CD8+ groups). A. The T1C map shows cystic changes within the tumor, with obvious enhancement of the cyst wall and surrounding edema; B. The method used to determine the ROI for obtaining the T1C histogram; C. The T1C histogram of the tumor mass. The T1C histogram parameter values were as follows: Minimum, 80; Maximum, 975; Mean, 2.555; SD, 1.391; Variance, 1.934; CV, 5.445; Skewness, 1.455; Perc.05, 114; Perc.10, 131; Perc.25, 169; Perc.50, 190; Perc.75, 319; D. CD8+ T cell count was 14 (HE, x 400).

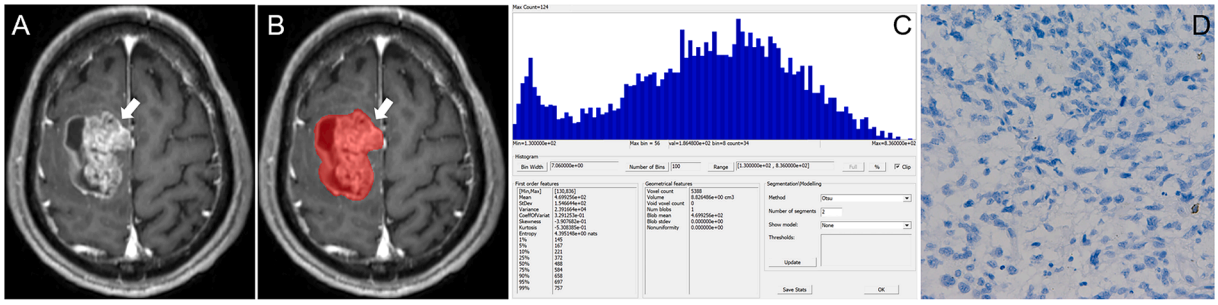

Fig. 2. A 54-year-old man with GBM in the right parietal lobe (Low CD8+ groups). A. The T1C map shows that the tumor is cystic and solid, with obvious enhancement; B. The method used to determine the ROI for obtaining the T1C histogram; C. The T1C histogram of the tumor mass. The T1C histogram values are as follows: Minimum, 130; Maximum, 836; Mean, 4.675; SD, 1.546; Variance, 2.391; CV, 3.308; Skewness, −3.427; Perc.05, 168; Perc.10, 226; Perc.25, 364; Perc.50, 484; Perc.75, 583; D. The CD8+ T cell count was 1 (HE, ×400).

2.6. Statistical analysis

Survival curves were drawn using Kaplan-Meier estimates; moreover, log-rank tests were used to analyze between-curve differences. The inter-observer reliability of T1C histogram parameters was assessed using the intra-class correlation coefficient (ICC), with an ICC index > 0.75 indicating high consistency. Normality and homoscedasticity of the measurement data were assessed using the one-sample Kolmogorov-Smirnov normality test and Levene test, respectively. Pearson's and Spearman's-Rho correlation analyses were used to analyze the relationship of T1C histogram parameters with the levels of CD8+ T cells. We performed two independent sample t-tests for each parameter in case of normal data distribution; otherwise, the Mann-Whitney *U* test was used. We performed receiver operating characteristic (ROC) analysis to evaluate the utility of the T1C histogram parameters in discriminating between the high and low CD8 expression groups. The area under the ROC curve (AUC) was calculated. The maximum Youden index was determined as the optimal threshold for distinguishing between the high and low expression groups. The AUC was expressed as the mean and 95% confidence interval. The pairwise AUC values for T1C histogram parameters were compared using the method by Delong et al.. The Bonferroni correction was used for multiple testing. All statistical analyses were performed using SPSS (IBM SPSS Statistics version 25.0; Chicago, IL, USA) and MedCalc (version 15.2; Ostend, Belgium) software.

3. Results

3.1. Patient grouping

We included 61 patients with GBM; among them, there were 24 (39.34%) and 37 (60.66%) patients in the high (CD8 > 2.6) and low (CD8 ≤ 2.6) CD8 expression groups, respectively (Fig. 3). Additionally, 18 and 16 patients in the high and low CD8 expression groups, respectively, died. There were significant between-group differences in the Kaplan-Meier curves (P = 0.0156).

3.2. Inter-observer agreement

The overall, mean, variance, and all percentile values showed excellent inter-reader agreement (ICC: 0.834–0.925); contrastingly, skewness, kurtosis, and entropy showed relatively low inter-reader agreement (ICC, 0.687, 0.703, and 0.717, respectively).

3.3. Correlation of T1C histogram parameters with CD8+ T cells

Table 1 and Fig. 4 show the correlations between the T1C histogram parameters and CD8+ T cell levels. The mean, 5th, 10th, 25th, and 50th percentiles were negatively correlated with CD8+ T cell levels (correlation coefficients: −0.271, −0.293, −0.333, −0.397, and −0.379, respectively; all P < 0.05). CV was positively correlated with CD8+ T cell levels (correlation coefficient: 0.479; P < 0.05).

3.4. Between-group comparisons of the T1C histogram parameters

Table 2 shows the results of T1C histogram parameter analysis in both groups. There were no significant between high (10.11 ± 4.51 cm^2) and low (10.74 ± 6.30 cm^2) CD8+ groups differences in the area of ROI (P < 0.05). There were significant between-group differences in the CV, 1st, 5th, 10th, 25th, and 50th percentiles (all P < 0.05); however, there were no significant between-group differences in the maximum, minimum, mean, SD, variance, as well as the 75th, 90th, 95th, and 99th (all P > 0.05). Typical cases are shown in Figs. 1 and 2.

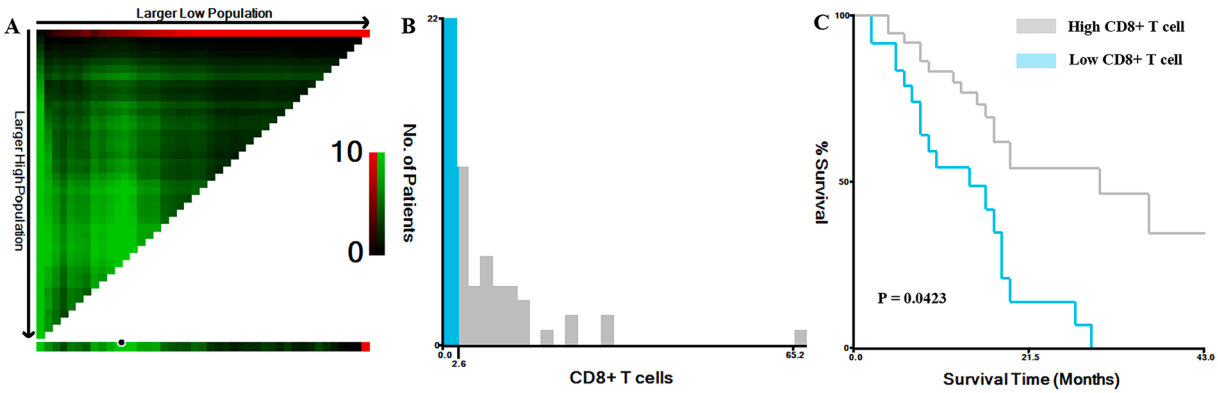

Fig. 3. X-tile plot showing the association between the levels of tumor-infiltrating CD8+ T cells and survival in patients with GBM. A: The plot color represents the strength of the association for each partition, ranging from low (dark, black) to high (bright, green). Green represents a direct association. B: The optimal cutoff value for CD8+ T cells was 2.6. C: The association between CD8+ T cells and overall survival (p = 0.0156). (For interpretation of the references to color in this figure legend, the reader is referred to the web version of this article.)

Table 1
Correlation between T1C histogram parameters and CD8 expression.

Parameter	CD8 expression	
	r	P
Minimum	−0.131	0.313
Maximum	−0.107	0.411
Mean	−0.271	0.035
SD	−0.153	0.239
Variance	−0.094	0.469
CV	0.479	<0.001
Skewness	0.037	0.777
Kurtosis	0.129	0.322
Entropy	−0.252	0.050
Perc.01	−0.251	0.051
Perc.05	−0.293	0.022
Perc.10	−0.333	0.009
Perc.25	−0.397	0.002
Perc.50	−0.379	0.003
Perc.75	−0.205	0.114
Perc.90	−0.099	0.449
Perc.95	−0.075	0.566
Perc.99	0.013	0.924

r indicates: Pearson correlation coefficient; SD: Standard deviation; CV: Coefficient of Variation.

3.5. ROC analysis of T1C histogram parameters for distinguishing between the low and high CD8 groups

Fig. 5 and Table 3 show the results of the ROC analysis of the T1C histogram parameters with significant between-group differences. The predictive AUC values for CV, 1st, 5th, 10th, 25th, and 50th percentiles were 0.783, 0.662, 0.706, 0.753, 0.681, and 0.725, respectively. Pairwise comparisons among these AUC values using the method developed by Delong et al. revealed no significant differences (all P > 0.0033).

4. Discussion

Our findings demonstrated that the level of GBM tumor-infiltrating CD8+ T cells was positively associated with the OS (P = 0.0156). Among the T1C histogram parameters, the mean as well as the 5th, 10th, 25th, and 50th percentiles were negatively correlated with the levels of CD8+ T cells. CV was positively correlated with the levels of CD8+ T cells. There were significant between-group differences in the CV as well as the 1st, 5th, 10th, 25th, and 50th percentiles. Our findings indicate that histograms can effectively reflect tumor heterogeneity and that T1C histogram parameters are feasible predictors of tumor-infiltrating CD8+ T cell levels in patients with GBM.

Immunotherapy has led to dramatic changes in the traditional

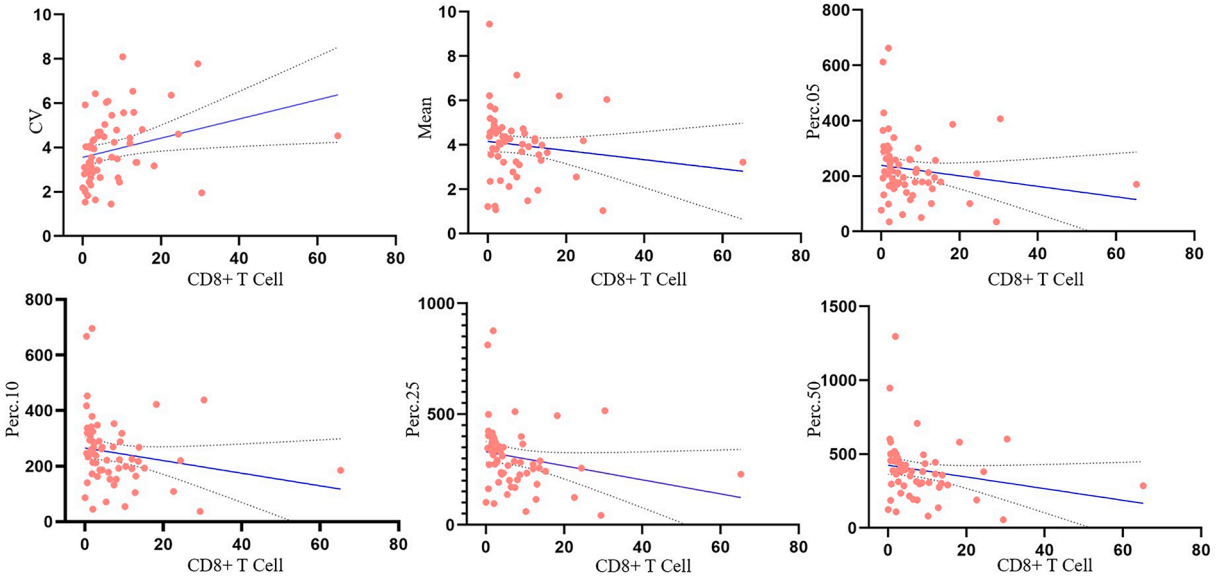

Fig. 4. Scatter plot showing significant correlations of the CV, mean, Perc.05, Perc.10, Perc.25, and Perc.50 values with tumor-infiltrating CD8+ T cell levels.

Table 2
T1C histogram parameters between Low-CD8 and High-CD8 Glioblastomas.

Parameter (mm^2/s)	Low-CD8 group (n = 24)	High-CD8 group (n = 37)	P value
Minimum	134.50(93.50, 174.25)	104.00(76.50, 141.00)	0.097
Maximum	1005.50(761.75, 1131.50)	897.00(764.50, 1105.00)	0.295
Mean	4.60(3.62, 5.03)	4.03(3.16, 4.37)	0.055
SD	1.64(1.34, 3.54)	1.76(1.36, 2.10)	0.802
Variance	2.54(1.83, 3.76)	2.86(1.85, 4.17)	0.734
CV	3.09(2.34, 3.50)	4.48(3.33, 5.51)	< 0.001
Skewness	1.85 ± 4.00	3.33 ± 3.45	0.132
Kurtosis	−1.13 ± 4.97	0.39 ± 5.80	0.293
Entropy	4.09(3.88, 4.30)	4.03(3.84, 4.19)	0.275
Perc.01	213.00(144.75, 273.50)	161.00(142.00, 191.00)	0.034
Perc.05	260.50 (175.75,308.50)	179.00(154.00, 232.50)	0.017
Perc.10	285.50(218.00, 340.00)	199.00(163.50, 268.00)	0.007
Perc.25	367.00(289.75, 412.00)	253.00(196.50, 301.50)	0.001
Perc.50	454.50(366.50, 506.50)	358.00(281.00, 425.50)	0.003
Perc.75	454.50(366.50, 506.50)	493.00(377.00, 565.50)	0.159
Perc.90	630.00(537.25, 688.50)	611.00(500.50,711.00)	0.550
Perc.95	698.00(599.50, 777.00)	650.00(558.50, 782.00)	0.679
Perc.99	819.50(682.00, 926.75)	829.00(671.50, 904.00)	0.848

SD: Standard deviation; CV: Coefficient of Variation.

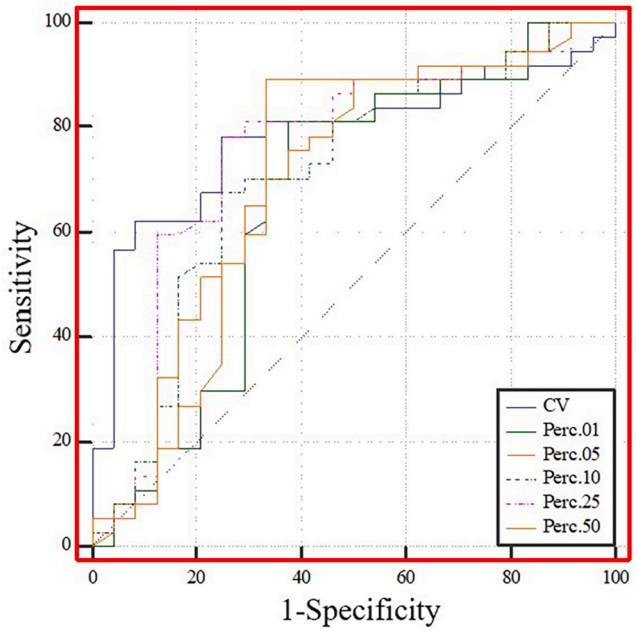

Fig. 5. ROC curve analysis of T1C histogram parameters to distinguish between the low and high CD8 expression groups. The predictive AUC values for CV, 1st, 5th, 10th, 25th, and 50th percentiles were 0.783, 0.662, 0.706, 0.753, 0.681, and 0.725, respectively.

treatment strategies for cancer (Ansell, 2016). However, the efficacy of immunotherapy is mainly affected by the TME phenotype, especially the levels of tumor-infiltrating CD8+ T cells, which are positively correlated with the efficacy of immunotherapy and survival (Tong et al., 2022). T1C is a routine scan sequence for brain tumor patients, and it is more widely used in the diagnosis and evaluation of brain tumor patients at all levels of hospitals than the advanced functional MRI methods, such as

Table 3
ROC analysis of T1C histogram parameters for distinguishing CD8 expression status.

	Youden index	Cutoff	Sensitivity (%)	Specificity (%)	AUC (95% CI)
CV	0.534	3.32	78.40	75.00	0.783 (0.658–0.878)
Perc.01	0.436	200.50	62.50	81.10	0.662 (0.529–0.778)
Perc.05	0.392	261.50	50.00	89.20	0.681 (0.550–0.795)
Perc.10	0.426	229.00	75.00	67.60	0.706 (0.576–0.816)
Perc.25	0.534	313.50	75.00	78.40	0.753 (0.626–0.854)
Perc.50	0.559	444.50	66.70	89.20	0.725 (0.595–0.831)

CV: Coefficient of Variation ; ROC: Receiver operating characteristic; AUC: Area under the ROC curve; CI: Confidence interval.

DWI, PWI, APT, etc., and is more easily accessible than other scan sequences. In addition, T1WI-enhanced imaging can, to some extent, reflect the anatomical, blood supply and cellular component information of the lesion while fully demonstrating the internal features of the lesion and more clearly showing the lesion boundary compared to other conventional scan sequences (Kandemirli et al., 2020; Zhou et al., 2017). CD8 T cells have the capacity to initiate astrocyte activation, cerebral endothelial cell tight junction protein alterations and CNS vascular permeability through a perforin-dependent process (Suidan et al., 2010). Increased microvascular permeability and easier access of contrast agents to tumor tissue may cause GBM to exhibit different degrees of enhancement in T1C. Therefore, T1C histogram parameters could differentiate between low and high CD8 expression; accordingly, preoperative histogram analysis could inform appropriate patient treatment or follow-up plans before biopsy or surgery.

Histogram analysis converts the grayscale information of each pixel in the image into frequency distribution information, with the histogram feature parameters being used for quantitative analysis (Just, 2014). Specifically, these parameters, which are among the basic statistical features in radiomics, can quantitatively reflect the data distribution. Compared with traditional methods, histogram analysis can better reflect the internal tumor information through statistical analysis of the distribution characteristics of the parameters. Tumor heterogeneity is a specific feature of tumor progression and malignancy together with necrosis, high cell density, hemorrhage, angiogenesis, etc. (Nelson et al., 2004). Most studies have applied manual delineation of the entire tumor for histogram analysis, which may be more objective and better reflect the lesion heterogeneity. However, whole-tumor histogram analysis may not be practical in daily clinical practice given its cumbersomeness. Our histogram analysis was based on the largest tumor cross-section on the T1C images. Although some information regarding the remaining tumor may be lost, this method is simpler, faster, and more clinically useful. Conventional T1WI and T2WI cannot sufficiently reflect tumor heterogeneity; contrastingly, T1C imaging can reflect GBM heterogeneity and is related to prognosis (Yildirim and Baykara, 2022). Therefore, the use of T1C histogram parameters to analyze CD8+ T cell levels in GBM has great potential.

Percentile is the most widely used parameter in histogram analysis. In our study, there was a significant between-group difference in the 1st, 5th, 10th, 25th, and 50th percentiles; however, there was no significant between-group difference in the mean values. This indicates that the percentile can better reflect the internal lesion characteristics. The CV describes the degree of dispersion of the means of the characteristic values of the lesions. A larger CV indicates more deviation of the data from the mean value, and thus greater variability of the lesions (Shi et al., 2020). In our study, the CV values were significantly higher in the high CD8 expression group than in the low CD8 expression group, which

indicates an uneven mean distribution of lesion characteristics in the CD8 group, and thus lesion variability. Further studies are warranted to confirm this.

4.1. Limitations

This study has several limitations. First, this was a small-scale single-center study. Second, we manually drew the ROI on the largest lesion slice, which may not accurately reflect the characteristics of the entire tumor. Third, we did not consider multimodal MRI indicators, including DTI, DKI, PWI, etc. Fourth, we did not consider PD-1, PD-L1, and cytotoxic T lymphocyte-associated protein 4, which negatively regulate T cell function.

5. Conclusion

MRI histogram analysis is a non-invasive imaging method with promising implications in the preoperative prediction of tumor-infiltrating CD8+ T cell levels in patients with GBM.

CRediT authorship contribution statement

Caiqiang Xue: Conceptualization, Methodology, Writing – original draft. **Qing Zhou:** Investigation. **Peng Zhang:** Investigation. **Bin Zhang:** Formal analysis. **Qiu Sun:** Writing – review & editing. **Shenglin Li:** Formal analysis. **Juan Deng:** Investigation. **Xianwang Liu:** Writing – review & editing. **Junlin Zhou:** Resources, Visualization, Project administration.

Declaration of Competing Interest

The authors declare that they have no known competing financial interests or personal relationships that could have appeared to influence the work reported in this paper.

Data availability

Data will be made available on request.

Acknowledgements

Thanks to all the partners who contributed to this research, including Caiqiang Xue, Qing Zhou, Peng Zhang, Bin Zhang, Qiu Sun, Shenglin Li, Juan Deng, Xianwang Liu.

Funding

This work was supported by National Natural Science Foundation of China (grant number 82071872).

References

Ansell, S.M., 2016. Hodgkin lymphoma: MOPP chemotherapy to PD-1 blockade and beyond. Am. J. Hematol. 91, 109–112.

Apetoh, L., Smyth, M.J., Drake, C.G., Abastado, J.P., Apte, R.N., Ayyoub, M., Blay, J.Y., Bonneville, M., Butterfield, L.H., Caignard, A., Castelli, C., Cavallo, F., Celis, E., Chen, L., Colombo, M.P., Comin-Anduix, B., Coukos, G., Dhodapkar, M.V., Dranoff, G., Frazer, I.H., Fridman, W.H., Gabrilovich, D.I., Gilboa, E., Gnjatic, S., Jager, D., Kalinski, P., Kaufman, H.L., Kiessling, R., Kirkwood, J., Knuth, A., Liblau, R., Lotze, M.T., Lugli, E., Marincola, F., Melero, I., Melief, C.J., Mempel, T.R., Mittendorf, E.A., Odun, K., Overwijk, W.W., Palucka, A.K., Parmiani, G., Ribas, A., Romero, P., Schreiber, R.D., Schuler, G., Srivastava, P.K., Tartour, E., Valmori, D., van der Burg, S.H., van der Bruggen, P., van den Eynde, B.J., Wang, E., Zou, W., Whiteside, T.L., Speiser, D.E., Pardoll, D.M., Restifo, N.P., Anderson, A.C., 2015. Consensus nomenclature for CD8(+) T cell phenotypes in cancer. Oncoimmunology 4, e998538.

Bian, Y., Liu, Y.F., Jiang, H., Meng, Y., Liu, F., Cao, K., Zhang, H., Fang, X., Li, J., Yu, J., Feng, X., Li, Q., Wang, L., Lu, J., Shao, C., 2021. Machine learning for MRI radiomics: a study predicting tumor-infiltrating lymphocytes in patients with pancreatic ductal adenocarcinoma. Abdom Radiol. (NY) 46, 4800–4816.

Bian, Y., Liu, C., Li, Q., Meng, Y., Liu, F., Zhang, H., Fang, X., Li, J., Yu, J., Feng, X., Ma, C., Zhao, Z., Wang, L., Xu, J., Shao, C., Lu, J., 2022. Preoperative Radiomics Approach to Evaluating Tumor-Infiltrating CD8(+) T Cells in Patients With Pancreatic Ductal Adenocarcinoma Using Noncontrast Magnetic Resonance Imaging. J. Magn. Reson. Imaging 55, 803–814.

Davis, M.E., 2016. Glioblastoma: Overview of Disease and Treatment. Clin. J. Oncol. Nurs. 20, S2–S8.

Feng, P., Li, Y., Tian, Z., Qian, Y., Miao, X., Zhang, Y., 2022. Analysis of Gene Co-Expression Network to Identify the Role of CD8 + T Cell Infiltration-Related Biomarkers in High-Grade Glioma. Int. J. Gen. Med. 15, 1879–1890.

Gao, A., Zhang, H., Yan, X., Wang, S., Chen, Q., Gao, E., Qi, J., Bai, J., Zhang, Y., Cheng, J., 2022. Whole-Tumor Histogram Analysis of Multiple Diffusion Metrics for Glioma Genotyping. Radiology 302, 652–661.

Ghouzlani, A., Kandoussi, S., Tall, M., Reddy, K.P., Rafii, S., Badou, A., 2021. Immune Checkpoint Inhibitors in Human Glioma Microenvironment. Front. Immunol. 12, 679425.

Hagiwara, A., Schlossman, J., Shabani, S., Raymond, C., Tatekawa, H., Abrey, L.E., Garcia, J., Chinot, O., Saran, F., Nishikawa, R., Henriksson, R., Mason, W.P., Wick, W., Cloughesy, T.F., Ellingson, B.M., 2022. Incidence, molecular characteristics, and imaging features of "clinically-defined pseudoprogression" in newly diagnosed glioblastoma treated with chemoradiation. J Neurooncol.

Han, S., Zhang, C., Li, Q., Dong, J., Liu, Y., Huang, Y., Jiang, T., Wu, A., 2014. Tumour-infiltrating CD4(+) and CD8(+) lymphocytes as predictors of clinical outcome in glioma. Br. J. Cancer 110, 2560–2568.

Jiang, L., Zhou, L., Ai, Z., Xiao, C., Liu, W., Geng, W., Chen, H., Xiong, Z., Yin, X., Chen, Y.C., 2022. Machine Learning Based on Diffusion Kurtosis Imaging Histogram Parameters for Glioma Grading. J. Clin. Med. 11.

Just, N., 2014. Improving tumour heterogeneity MRI assessment with histograms. Br. J. Cancer 111, 2205–2213.

Kandemirli, S.G., Chopra, S., Priya, S., Ward, C., Locke, T., Soni, N., Srivastava, S., Jones, K., Bathla, G., 2020. Presurgical detection of brain invasion status in meningiomas based on first-order histogram based texture analysis of contrast enhanced imaging. Clin. Neurol. Neurosurg. 198, 106205.

Lakin, N., Rulach, R., Nowicki, S., Kurian, K.M., 2017. Current Advances in Checkpoint Inhibitors: Lessons from Non-Central Nervous System Cancers and Potential for Glioblastoma. Front. Oncol. 7, 141.

Liu, D., Chen, J., Ge, H., Yan, Z., Luo, B., Hu, X., Yang, K., Liu, Y., Liu, H., Zhang, W., 2022a. Radiogenomics to characterize the immune-related prognostic signature associated with biological functions in glioblastoma. Eur. Radiol.

Liu, X., Wang, Y., Wei, J., Li, S., Xue, C., Deng, J., Liu, H., Sun, Q., Zhang, X., Zhou, J., 2022b. Role of diffusion-weighted imaging in differentiating angiomatous meningioma from atypical meningioma. Clin. Neurol. Neurosurg. 221, 107406.

Nelson, D.A., Tan, T.T., Rabson, A.B., Anderson, D., Degenhardt, K., White, E., 2004. Hypoxia and defective apoptosis drive genomic instability and tumorigenesis. Genes Dev. 18, 2095–2107.

Ren, X., Zhang, L., Zhang, Y., Li, Z., Siemers, N., Zhang, Z., 2021. Insights Gained from Single-Cell Analysis of Immune Cells in the Tumor Microenvironment. Annu. Rev. Immunol. 39, 583–609.

Shi, Z., Li, J., Zhao, M., Peng, W., Meddings, Z., Jiang, T., Liu, Q., Teng, Z., Lu, J., 2020. Quantitative Histogram Analysis on Intracranial Atherosclerotic Plaques: A High-Resolution Magnetic Resonance Imaging Study. Stroke 51, 2161–2169.

Suidan, G.L., Dickerson, J.W., Chen, Y., McDole, J.R., Tripathi, P., Pirko, I., Seroogy, K. B., Johnson, A.J., 2010. CD8 T cell-initiated vascular endothelial growth factor expression promotes central nervous system vascular permeability under neuroinflammatory conditions. J. Immunol. 184, 1031–1040.

Sun, Q., Chen, Y., Liang, C., Zhao, Y., Lv, X., Zou, Y., Yan, K., Zheng, H., Liang, D., Li, Z. C., 2021. Biologic Pathways Underlying Prognostic Radiomics Phenotypes from Paired MRI and RNA Sequencing in Glioblastoma. Radiology 301, 654–663.

Teng, M.W., Ngiow, S.F., Ribas, A., Smyth, M.J., 2015. Classifying Cancers Based on T-cell Infiltration and PD-L1. Cancer Res. 75, 2139–2145.

Tong, H., Sun, J., Fang, J., Zhang, M., Liu, H., Xia, R., Zhou, W., Liu, K., Chen, X., 2022. A Machine Learning Model Based on PET/CT Radiomics and Clinical Characteristics Predicts Tumor Immune Profiles in Non-Small Cell Lung Cancer: A Retrospective Multicohort Study. Front. Immunol. 13, 859323.

Ugel, S., Cane, S., De Sanctis, F., Bronte, V., 2021. Monocytes in the Tumor Microenvironment. Annu. Rev. Pathol. 16, 93–122.

Ulyte, A., Katsaros, V.K., Liouta, E., Stranjalis, G., Boskos, C., Papanikolaou, N., Usinskiene, J., Bisdas, S., 2016. Prognostic value of preoperative dynamic contrast-enhanced MRI perfusion parameters for high-grade glioma patients. Neuroradiology 58, 1197–1208.

Vajapeyam, S., Brown, D., Ziaei, A., Wu, S., Vezina, G., Stern, J.S., Panigrahy, A., Patay, Z., Tamrazi, B., Jones, J.Y., Haque, S.S., Enterline, D.S., Cha, S., Jones, B.V., Yeom, K.W., Onar-Thomas, A., Dunkel, I.J., Fouladi, M., Fangusaro, J.R., Poussaint, T.Y., 2022. ADC Histogram Analysis of Pediatric Low-Grade Glioma Treated with Selumetinib: A Report from the Pediatric Brain Tumor Consortium. AJNR Am. J. Neuroradiol. 43, 455–461.

Xu, M., Tang, Q., Li, M., Liu, Y., Li, F., 2021. An analysis of Ki-67 expression in stage 1 invasive ductal breast carcinoma using apparent diffusion coefficient histograms. Quant. Imaging Med. Surg. 11, 1518–1531.

Xue, C., Liu, S., Deng, J., Liu, X., Li, S., Zhang, P., Zhou, J., 2022. Apparent Diffusion Coefficient Histogram Analysis for the Preoperative Evaluation of Ki-67 Expression in Pituitary Macroadenoma. Clin. Neuroradiol. 32, 269–276.

Yang, I., Tihan, T., Han, S.J., Wrensch, M.R., Wiencke, J., Sughrue, M.E., Parsa, A.T., 2010. CD8+ T-cell infiltrate in newly diagnosed glioblastoma is associated with long-term survival. J. Clin. Neurosci. 17, 1381–1385.

Yildirim, M., Baykara, M., 2022. Differentiation of progressive disease from pseudoprogression using MRI histogram analysis in patients with treated glioblastoma. Acta Neurol. Belg. 122, 363–368.
Zhang, H.W., Lyu, G.W., He, W.J., Lei, Y., Lin, F., Feng, Y.N., Wang, M.Z., 2020. Differential diagnosis of central lymphoma and high-grade glioma: dynamic contrast-enhanced histogram. Acta Radiol. 61, 1221–1227.
Zhou, X., Qu, M., Tebon, P., Jiang, X., Wang, C., Xue, Y., Zhu, J., Zhang, S., Oklu, R., Sengupta, S., Sun, W., Khademhosseini, A., 2020. Screening Cancer Immunotherapy: When Engineering Approaches Meet Artificial Intelligence. Adv. Sci. (Weinh) 7, 2001447.
Zhou, W., Zhang, L., Wang, K., Chen, S., Wang, G., Liu, Z., Liang, C., 2017. Malignancy characterization of hepatocellular carcinomas based on texture analysis of contrast-enhanced MR images. J. Magn. Reson. Imaging 45, 1476–1484.